OPTIMIZATION OF DISCHARGE PATTERNS IN PARKINSON CONDITION IN SUBTHALAMIC NUCLEUS MODEL OF BASAL GANGLIA USING PARTICLE SWARM OPTIMIZATION ALGORITHM

SHRI DHAR[1], SANJAY YADAV, PHOOL SINGH, JYOTSNA SINGH, AND A. K. YADAV

ABSTRACT. Parkinson disease is a well-known movement disorder in which production of dopamine in the brain reduces. In this paper, we have considered a conductance - based model of subthalamic nucleus and globus pallidus (external) for a primate suffering from Parkinson disease. Discharge patterns from the model are first recorded for normal condition primate and with Parkinson disease. Thereafter, we have applied particle swarm optimization algorithm to various membrane potentials such as calcium (V_{Ca}), feedback neuron to STN (V_{fs}), potassium (V_K) and sodium (V_{Na}) so that Parkinson primate's discharge patterns mimic the discharge patterns of healthy primate. A qualitative comparison between the discharge patterns of healthy and optimized Parkinson primate is made by computing correlation coefficient for different time spans (up to 750 msec) which turns out to be more than 0.9981 in each case. The value being very close to 1 indicates a very high-degree of overlap of the two patterns.

1. INTRODUCTION

Brain disorders are increasingly becoming a serious issue and their study is a major challenge for the scientific community [1–3]. The lack of proper understanding of these disorders is a major hurdle in developing quality diagnostic

systems for their early detection. A well-known brain disorder which mainly affects the movement of body parts is known as Parkinson Disease (PD). The most affected part of the brain in Parkinson disease is Substantia Nigra Pars Compacta [4–7]. Neurons present in this area of the brain get affected in Parkinson disease. These neurons are responsible for production of dopamine, a chemical which takes care of the messages to control the movement of the primate's body. With the passage of time, production of dopamine decreases, resulting in loss of control of the PD primate over the movement process. When the symptoms are clearly visible, the treatment of Parkinson disease is available [8–11]. However the real cause of decrease in production of dopamine is not yet established, thus hampering the prevention of Parkinson disease in its early stages. Basal ganglia mainly consists of four nuclei: a) Subthalamic Nucleus (STN), b) Striatum, c) Substantia Nigra - further classified into two parts i) Pars Compacta, and ii) Pars Reticulata, d) Globus Pallidus (GP) which is also of two types i) Internal Globus Pallidus (GPi), and ii) External Globus Pallidus (GPe). Cortex gives input to the striatum directly which transfers it to GP (internal as well as external). Transfer from striatum to GP is through direct and indirect pathways. Cortex gives input to STN as well but this input is given by hyper direct pathways [12–16]. Direct pathways and indirect pathways control the unconstrained movement as they affect the network of basal ganglia in opposite manner [17–21].

In the recent past, several researchers have narrow down their study to the origin of Parkinson disease [22–31], and could identify the possible causes of its occurrence. However, no success has been achieved in ascertaining specific cause for a given primate. While studying oscillations and bursting in the circuits of basal ganglia [32–42], it was established that subthalamic nucleus (STN) is responsible for motor function and calcium current (ICa) plays a vital role in the proper functioning of STN neuron. In an attempt to determine the factors responsible for tremor and bursting, we consider a model shown in Figure 1 (the dotted lines represents inhibitory synapse while the arrow represents excitatory synapses and the connections are shown as bold lines for healthy and as dotted lines for Parkinson disease primate).

During 1970s, Back Propagation (BP) algorithm or its derivative was a major tool to optimize any model with linear or non-linear functions. But the problems with this algorithm were related to the selection of initial set of values and regarding the fluctuation or overflow of calculations instead of attaining the
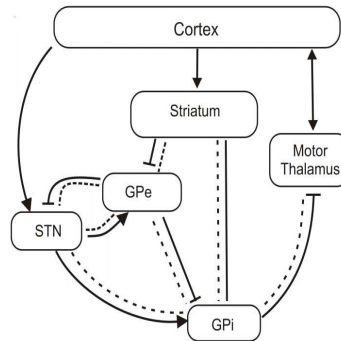
FIGURE 1. Modified Basal ganglia-thalamo-cortical circuit [43]

optimum value(s). To overcome these problems, an effective technique known as particle swarm optimization (PSO) algorithm, was proposed by Eberhart and Kennedy in 1995 [44]. Particle swarm optimization (PSO) is a well-known technique used by researchers for optimization purposes. The central idea of PSO algorithm is drawn from a flock of birds that learn through communication while searching for food. In this process, the flock identifies the bird which is at the best position and accordingly the whole flock manages to reach there and this process is repeated till they reach their ultimate destination.

Over the years, particle swarm optimization is finding extensive implementation in a variety of models. In 2005, the performance of particle swarm optimization algorithm was compared with other evolutionary algorithms (EAs) [45]. Non-linear problems were optimized by using particle swarm optimization algorithm in 2006 [46] with a high degree of accuracy. In another study, PSO algorithm was successfully implemented to optimize the diameter errors in a boring machine [47]. Though PSO algorithm has been implemented successfully in a large number of models, a few notable ones are [48–51].

In 2007, Feng et al. optimized deep brain simulation patterns using genetic algorithm (GA) [52] in the STN model. In a recent study by Singh et al., the sensitivity analysis of subthalamic nucleus in a model taken for basal ganglia has been carried out [43]. They discussed that the discharge patterns generated for a Parkinson disease primate depends mainly on four membrane potentials which are $V_{Ca}, V_{fs}, V_{Na}, V_k$ but are most sensitive for V_{Ca}, i.e. for calcium membrane potential. They have optimized calcium membrane potential in their study and

suggested that the two discharge patterns (healthy and Parkinson primate) will have high similarity for V_{Ca}=235 mV and the value of correlation coefficient for this membrane potential obtained by them was 0.92. They have applied linear search algorithm to optimize the various member potentials by considering one at a time. Their study for calcium membrane potential motivated us to implement particle swarm optimization algorithm to determine the optimal solution by considering all the four membrane potentials simultaneously.

This paper is organized as follows: Section 2 describes the model of basal ganglia to optimize membrane potentials for a Parkinson disease primate. Section 3 explains the particle swarm optimization algorithm. Section 4 is dedicated to the implementation of particle swarm optimization and the results. Finally, the conclusions of the study are given in section 5.

2. Model of Basal Ganglia

This study is based on a single-compartment conductance-based model [18] in which cortex sends excitatory input through hyper-direct pathway to STN [20] and STN sends excitatory input to GPe (shown by arrows in Figure 1). Also striatum sends inhibitory input to GPe and GPe sends inhibitory input to STN (shown by bars in Fig. 1). In this model, STN receives inputs from cortex and GPe, which results in an increase in the frequency of discharge patterns in GPi neurons [53, 54] and this is responsible for the interaction of GP neuron and STN in direct pathway as well as hyper-direct pathway [18, 55]. Other than mathematical model, we have to consider conductance and time scale to analyze the activity patterns in subthalamic nucleus network in a healthy and PD primate [56]. The simulation and analysis of this model for optimization of membrane potentials is performed using MATLAB 7.16 (over 4 GB RAM Machine and i7 Intel processor) with ODE45. Time spam is taken up to 750 msec while performing the analysis.

The membrane potential (V) in this model includes a leak current (I_l), fast spike producing potassium (I_k) and sodium(I_{Na}) currents, low threshold T-type (I_T) high-threshold Ca^{2+} currents (I_{Ca}), Ca^{2+} activated voltage independent after-hyperpolarization K^+current (I_{AHP}), synaptic current(I_{syn}) and applied

current (I_{app}) and can be written in the form [22]:

(2.1) $$C\frac{dV}{dt} = -I_l - I_k - I_{Na} - I_T - I_{Ca} - I_{AHP} - I_{syn} + I_{app}$$

where the membrane currents are governed by the following equations:

$$I_l = g_l.[V - V_l]$$

$$I_k = g_k n^4 [V - V_k]$$

$$I_{Na} = g_{Na} m_\infty^3(V).h.[V - V_{Na}]$$

$$I_T = g_T a_\infty^3(V).r.[V - V_{Ca}]$$

$$I_{Ca} = g_{Ca} s_\infty^3(V).[V - V_{Ca}]$$

$$I_{AHP} = g_{AHP}.\frac{[Ca]}{[Ca] + k_1}[V - V_{Ca}]$$

where k_1 is the dissociation constant of I_{AHP} and applied current (I_{app}) is to adjust the resting potential of the values measured during the experiment [57]. The calcium current is determined by the following equation:

$$\frac{d[Ca]}{dt} = \epsilon[-I_{Ca} - I_T - k_{Ca}[Ca]])$$

where the constant ϵ is the calcium flux, k_{Ca} characterizes the pump rate of calcium and the variables n, h, r, m, s and a can be obtained from the following equation:

$$\frac{dx}{dt} = \frac{\phi_x[x_\infty(V) - x]}{(\tau_x(V)}$$

Here, ϕ_x is simply a constant for the gating variables, and τ_x which is a function of V represents time constant function represented by the equation:

$$\tau_x(V) = \tau_x^0 + \frac{\tau_x^1}{1 + exp(-\frac{V - \theta_x^\tau}{\sigma_x^\tau})}$$

where the values of τ_x^0, τ_x^1, θ_x^τ and σ_x^τ can be taken from the appendix taken from [58] (given at the end of the paper) and hence τ_x will be a function of V only for $x = n, h, r, m, s, a$.

Also, $x_\infty(V)$ which represents steady-state voltage dependence is given by:

$$x_\infty(V) = \frac{1}{1 + \exp(-\frac{[V - \theta_x]}{\sigma_x})}$$

where θ_x is half activation or inactivation voltage and σ_x is slope factor for x (gating variable). I_{syn} (synaptic current) is obtained by taking the sum of synaptic current from GPe and the other neighboring neuron [56], that is, it is taken by considering synaptic conductance from GPe to STN denoted by g_{gs}, synaptic conductance from feedback neuron to STN denoted by g_{fs}, membrane potentials from GPe to STN(V_{gs}) and from feedback neuron to STN(V_{fs}), and synaptic variables s_g and s_f in the following way:

$$I_{syn} = g_{gs}.s_g.[V - V_{gs}] + g_{fs}.s_f.[V - V_{fs}]$$

As mentioned in [22], Parkinson disease is mainly caused by the degeneration of dopamine and this dopamine degeneracy can be majorly shown by synaptic input variables s_g and s_f which can be obtained by the following equation:

$$\frac{ds_i}{dt} = \alpha.H_\infty(V).(V_{presyn} - \theta_g).[1 - s_i] - \beta s_i$$

for $i = g, s$, where β, V_{presyn}, θ_g can be taken from [58, 59] (values are given in the appendix) and $H_\infty(V)$ (sigmoid function) is given by the equation:

$$H_\infty(V) = \frac{1}{[1 + e^{\frac{-[V - \theta_g^H]}{\sigma_g^H}}]}$$

3. PARTICLE SWARM OPTIMIZATION ALGORITHM

Particle swarm optimization (PSO) [60] is an inhabitant based optimization method in which a group of elements move in search space to find the best solution for a given problem. The fundamental concept behind the particle swarm optimization algorithm is taken from the flock of birds that learn through communication while searching for food. In this process, the flock identifies the bird which is at the best position and accordingly the whole flock manages to reach there and this process is repeated till they reach their ultimate destination. While using PSO algorithm, an element of finest ability from the group of elements that we have taken into consideration is selected. The velocity of each particle considered in this algorithm depends on two factors: position of that element with finest ability and the personal best ability of the element. Here the term finest ability refers to the best performance of a particle. In case of the horde of birds, finest ability will refer the closeness of the birds from the source

(which is food in this case). So the bird which is closest to the source will be taken as the particle with finest ability. In this case, it should be noted that the birds are learning in both ways: self-experience (called local search) and from the other's experience (called global search).

Figure 2 describes the flowchart in which the steps are described to implement the particle swarm optimization algorithm:
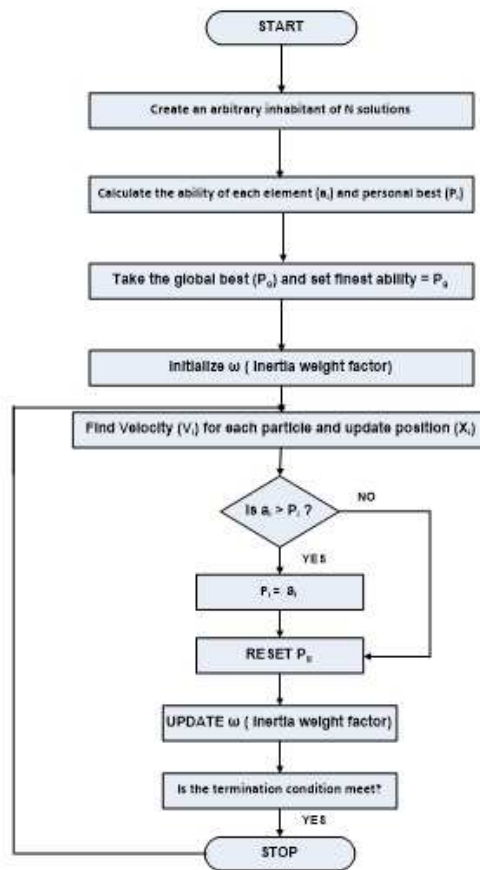

FIGURE 2. Flowchart of particle swarm optimization algorithm

The velocity and the updated position of each element can be calculated by the following equations:

$$v_{i,k}(t+1) = m \times v_{i,k}(t) + c_1 \times r_1 \times (P_{i,k} - x_{i,k}(t)) + c_2 \times r_2 \times ((P_g)_k - x_{i,k}(t))$$

$$x_{i,k}(t+1) = x_{i,k}(t) + v_{i,k}(t+1)$$

where $x_{i,k}$ and $v_{i,k}$ are the position and velocity of i-th particle when it is moving in k-th dimension, m is the momentum, c_1 and c_2 are constants, r_1 and r_2 are random variables that can take value from the segment $[0, 1]$.

4. Results and discussion

In this section, the spiking patterns obtained for a healthy primate are compared with the spiking patterns for a primate with PD in the model that we have taken into consideration. The values obtained may be different as they may vary from case to case [20]. We are denoting the spiking patterns generated in a health and PD primate by $(SP)_H$ and $(SP)_{PD}$ respectively. Now the comparison between $(SP)_H$ and $(SP)_{PD}$ is done by calculating correlation coefficient (CC) for these two which will tell us the likeness of two series as a function of lag of one comparative to the other. CC between $\{(SP)_H\}_t$ and $\{(SP)_{PD}\}_{t+i}$ gives us the ith order cross-correlation of $(SP)_H$ and $(SP)_{PD}$. CC_i (sample estimate of correlation coefficient) is given by:

$$CC_i = \frac{\sum_{j=1}^{n-i}(\{(SP)_H\}_j - (\bar{SP})_H)(\{(SP)_{PD}\}_{i+j} - (\bar{SP})_{PD})}{\sqrt{\sum_{j=1}^{n}(\{(SP)_H\}_j - (\bar{SP})_H)^2 \sum_{j=1}^{n}(\{(SP)_{PD}\}_j - (\bar{SP})_{PD})^2}}$$

Before investigating this model, different activity patterns generated by using equation (2.1) have been studied and it was found that the simulation for the patterns have been done for selected parameters for a time span of 250 ms and 500 ms respectively. The model is considerably sensitive for few parameters $(V_{Ca}, V_{fs}, V_{Na}, V_k)$ which we have taken into consideration and optimum values of these parameters have been identified simultaneously by using PSO algorithm. The way these parameters (membrane potentials) are attaining the optimum values is shown in the Figures 3(a)-3(d), 4(a)-4(d), 5(a)-5(d) and 6(a)-6(d) for different time spans up to 750 msec. The validation of the optimum values of membrane potential is done by generating the discharge patterns for PD primate after considering these optimized values. The resulting discharge patterns obtained for PD primate show a near perfect similarity with those of healthy primate as shown in Figures 3(f), 4(f), 5(f) and 6(f). A qualitative comparison is made by computing correlation coefficient (CC) between the two discharge patterns which turns out to be more than 0.9981 in each case as shown in Figures 3(e), 4(e), 5(e) and 6(e).
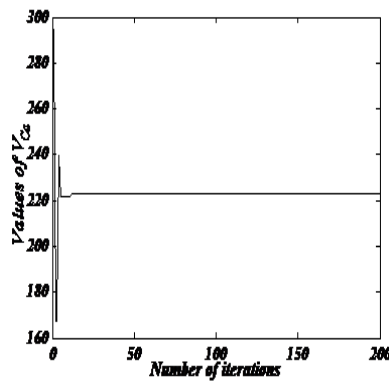
(a) For time span of 250 msec

FIGURE 3(a) Variation in the values of
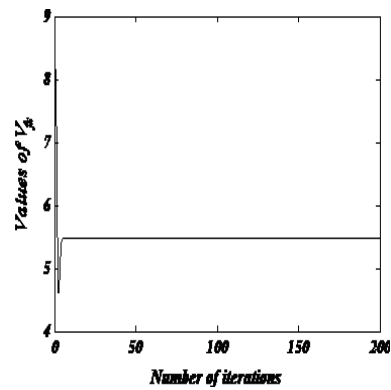V_{Ca} for 200 iterations
of PSO for 250 msec.

FIGURE 3(b) Variation in the values of
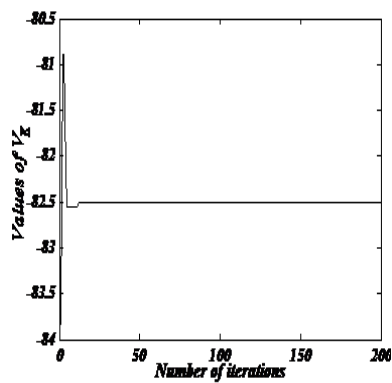V_{fs} for 200 iterations
of PSO for 250 msec.

FIGURE 3(c) Variation in the values
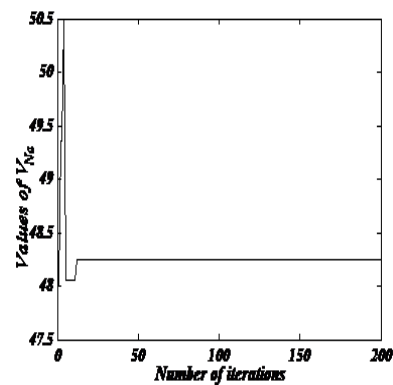of V_K for 200 iterations
of PSO for 250 msec.

FIGURE 3(d) Variation in the values
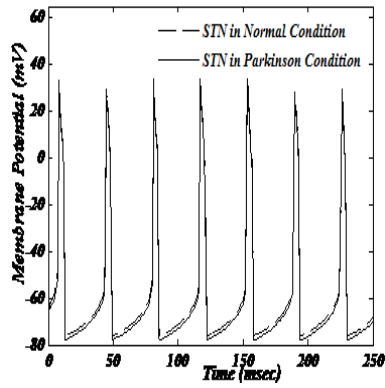of V_{Na} for 200 iterations
of PSO for 250 msec.

FIGURE 3(e) Discharge pattern for 250
msec for optimized values of V_{Ca},
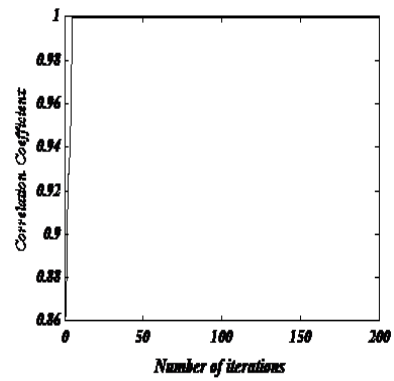V_{fs}, V_{Na} and V_k.

FIGURE 3(f) Correlation Coefficient
for 200 iterations of
PSO for 250 msec.

From the Figures 3(a)-3(d), the optimum values of four membrane potentials are V_{Ca}=222.8682 mV, V_{fs}=5.4880 mV, V_{Na}=48.2415 mV, V_k=-82.5063 mV. Figure 3(e) is validating the optimum values of membrane potentials as the two patterns are showing a very high degree of overlap. Figure 3(f) is showing that correlation coefficient is attaining a value 0.9995.

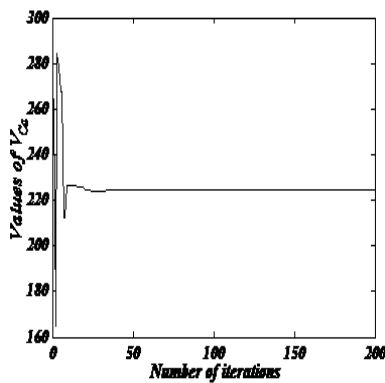(b) For time span of 500 msec

FIGURE 4(a) Variation in the values
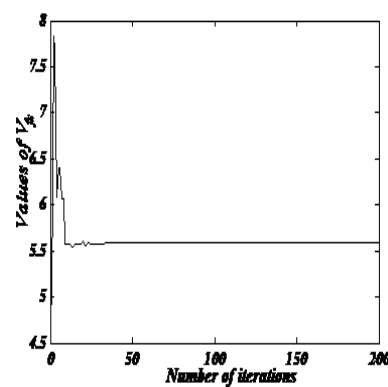of V_{Ca} for 200 iterations
of PSO for 500 msec.

FIGURE 4(b) Variation in the values
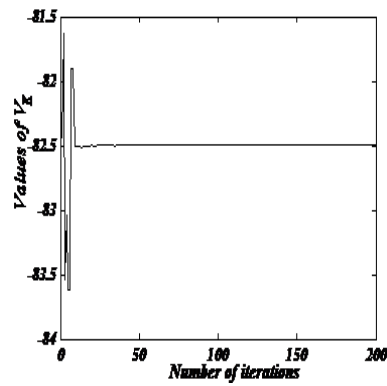of V_{fs} for 200 iterations
of PSO for 500 msec.

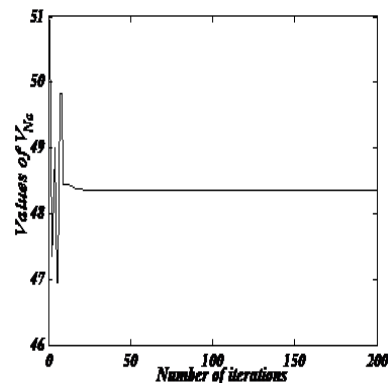FIGURE 4(c) Variation in the values of V_K for 200 iterations of PSO for 500 msec. of PSO for 500 msec.

FIGURE 4(d) Variation in the values of V_{Na} for 200 iterations of PSO for 500 msec.

FIGURE 4(e) Discharge pattern for 500 V_K for 200 iterations of PSO for 500 msec.
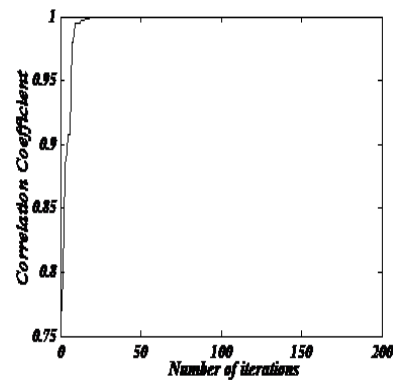
FIGURE 4(f) Correlation Coefficient for 200 iterations of PSO for 500 msec.

From the Figures 4(a)-4(d), the optimum values of four membrane potentials are V_{Ca}=224.3552 mV, V_{fs}=5.5832 mV, V_{Na}=48.3602 mV, V_k=-82.4983 mV. Figure 4(e) is validating the optimum values of membrane potentials as the two patterns are showing a very high degree of overlap. Figure 4(f) is showing that correlation coefficient is attaining a value 0.9994.

(c) For time span of 750 msec
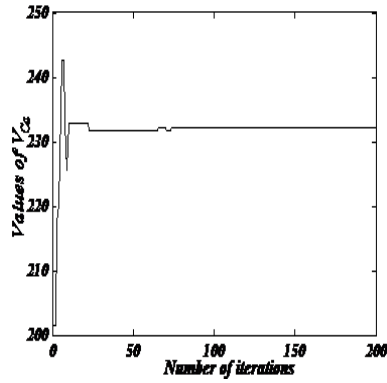
FIGURE 5(a) Variation in the values of V_{Ca} for 200 iterations of PSO for 750 msec.
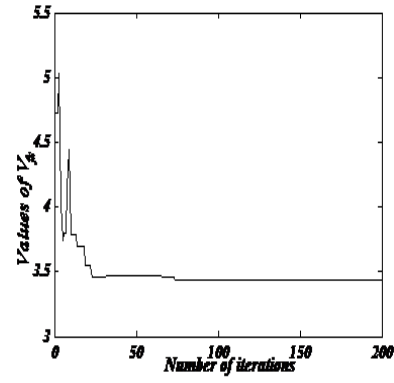
FIGURE 5(b) Variation in the values of V_{fs} for 200 iterations of PSO for 750 msec.
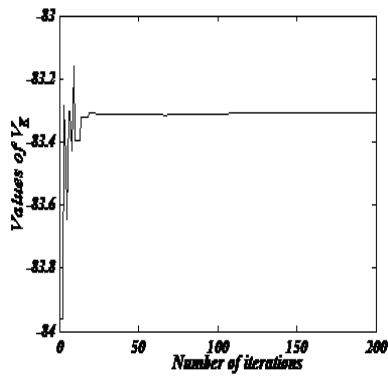
FIGURE 5(c) Variation in the values of V_K for 200 iterations of PSO for 750 msec.
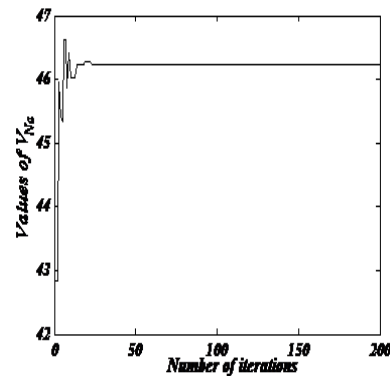
FIGURE 5(d) Variation in the values of V_{Na} for 200 iterations of PSO for 750 msec.

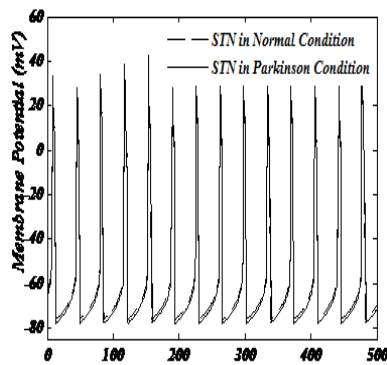From the Figures 5(a)-5(d), the optimum values of four membrane potentials are V_{Ca}=232.2110 mV, V_{fs}=3.4387 mV, V_{Na}=46.2448 mV, V_k=-83.3110 mV. Figure 5(e) is validating the optimum values of membrane potentials as the two patterns are showing a very high degree of overlap. Figure 5(f) is showing that correlation coefficient is attaining a value 0.9981.

FIGURE 5(e) Discharge pattern for 750 msec for optimized values of $V_{Ca}, V_{fs},$ V_{Na} and V_k.

FIGURE 5(f) Correlation Coefficient for 200 iterations of PSO for 750 msec.

The above results shown in the Figures 3(a)-3(d), 4(a)-4(d), 5(a)-5(d) shows the performance of the PSO algorithm as we are showing 200 iterations for each time span but the optimum values are obtained after 12 to 15 iterations only. It indicates the fast convergence for each of the membrane potential that we have taken into consideration. The 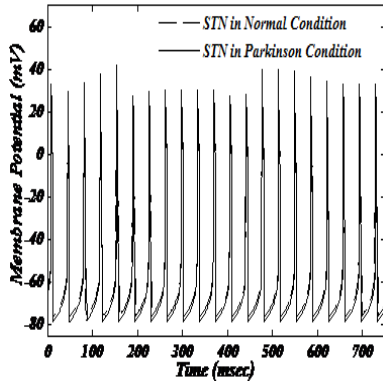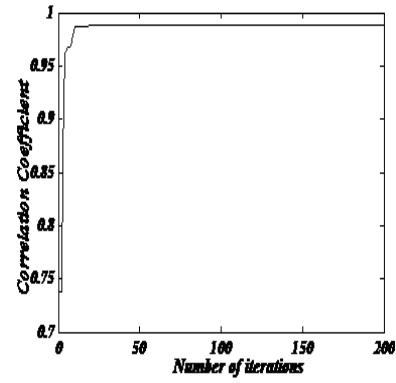Figures 3(e), 4(e) and 5(e) are validating the model for the optimum values of membrane potential obtained by using particle swarm optimization algorithm as the discharge pattern generated for a prime with Parkinson disease has very high degree of overlap with that of a healthy primate. Also, the Figures 3(f), 4(f) and 5(f) are representing the correlation coefficient taken for the discharge patterns of Parkinson disease primate and a healthy primate. The value of correlation coefficient which is close to 1 validates the optimality of the membrane potentials quantitatively. These results are giving us better results over the time span up to 750 msec as compared to the results obtained by the study of Singh et al. [43] in which the time span up to 250 msec was taken into consideration for the optimum value of calcium membrane potential to generate the discharge patterns for PD primate.

5. CONCLUSION

In this study, particle swarm optimization algorithm has been implemented to optimize the four membrane potentials in conductance-based model of subthalamic nucleus and globus pallidus for a Parkinson disease primate. This novel

approach has been used for the first time for parameter (membrane potentials) optimization in such a study on Parkinson disease primate. The results have been validated by correlation coefficient between the discharge patterns of healthy and Parkinson disease primate for various time spans up to 750 msec. The near-perfect results as shown by the overlapping discharge patterns also validate the model. Results of the present study show a significant improvement over the corresponding results reported in a recent study by Singh et al. [43]. Our results have been computed for time span of 750 msec, three times the time span taken (250 msec) by Singh et al. [43].

APPENDIX

Here we will define all the parameters used in the paper along with their units as follows:

$g_l = 2.25 nS/\mu m^2$ $g_k = 45 nS/\mu m^2$ $g_{Na} = 37.5 nS/\mu m^2$

$g_T = 0.5 nS/\mu m^2$ $g_{Ca} = 0.5 nS/\mu m^2$ $g_{APH} = 9 nS/\mu m^2$

$g_{syn} = 0.9 nS/\mu m^2$ $V_l = -60 mV$ $V_k = -80 mV$

$V_{Na} = 55 mV$ $V_{Ca} = 140 mV$ $V_s yn = -100 mV$

$\tau_n^1 = 100 msec$ $\tau_h^1 = 500 msec$ $\tau_r^1 = 17.5 msec$

$\tau_n^0 = 1 msec$ $\tau_h^0 = 1 msec$ $\tau_r^0 = 40 msec$

$\phi_n = 0.75$ $\phi_h = 0.75$ $\phi_r = 0.2$

$k_1 = 15$ $k_{Ca} = 22.5$ $\theta_n = -32$

$\theta_m = -30$ $\theta_h = -39$ $\theta_r = -67$

$\theta_a = -63$ $\theta_b = 0.4$ $\theta_s = -39$

$\theta_n^\tau = -80$ $\theta_h^\tau = -57$ $\theta_r^\tau = 68$

$\theta_g^H = -39$ $\theta_g = 30$ $\sigma_n = 8$

$\sigma_m = 15$ $\sigma_h = -3.1$ $\sigma_r = -2$

$\sigma_a = 7.8$ $\sigma_b = -0.1$ $\sigma_s = 8$

$\sigma_n^\tau = -26$ $\sigma_h^\tau = -3$ $\sigma_r^\tau = -2.2$

$\sigma_g^H = 8$ $\epsilon = 3.5 \times 10^{-5} m/sec$ $\alpha = 5 m/sec$

$\beta = 1.0 m/sec$ $g_{gs} = 0.695$ $g_{fs} = 0.215$

$V_{gs} = 5$ $V_{fs} = 5$ $C = 1$

$m = 0.8$ $c_1 = 1.4$ $c_2 = 2$

References

[1] B. J. Deacon: *The biomedical model of mental disorder: A critical analysis of its validity, utility, and effects on psychotherapy research*, Clin. Psychol. Rev., **33**(7) (2013), 846–861.

[2] D. Silberberg, N. P. Anand, K. Michels, R. N. Kalaria: *Brain and other nervous system disorders across the lifespan - global challenges and opportunities*, Nature, **527**(7578) (2015), S151–S154.

[3] G. Panuccio, M. Semprini, L. Natale, S. Buccelli, I. Colombi, M. Chiappalone: *Progress in Neuroengineering for brain repair: New challenges and open issues*, Brain Neurosci. Adv., **2**(2018), 1–11.

[4] Z. C. Baquet, P. C. Bickford, K. R. Jones: *Brain-Derived Neurotrophic Factor Is Required for the Establishment of the Proper Number of Dopaminergic Neurons in the Substantia Nigra Pars Compacta*, J. Neurosci., **25**(26) (2005), 6251–6259.

[5] W. R. W. Martin, M. Wieler, M. Gee: *Midbrain iron content in early Parkinson disease*, Neurology, **70**(16) (2008), 1411–1417.

[6] H. Takahashi et al.: *Comprehensive MRI quantification of the substantia nigra pars compacta in Parkinson's disease*, Eur. J. Radiol., **109**(2018), 48–56.

[7] A. G. Yee et al.: *Action potential and calcium dependence of tonic somatodendritic dopamine release in the Substantia Nigra pars compacta*, J. Neurochem., **148**(4) (2019), 462–479.

[8] H. Bergman et al.: *Physiological aspects of information processing in the basal ganglia of normal and parkinsonian primates*, Trends Neurosci., **21**(1) (1998), 32–38.

[9] M. M. Goldenberg: *Medical Management of Parkinson's Disease*, Pharm. Ther., **33**(10) (2008), 590–606.

[10] R. F. Pfeiffer: *Gastrointestinal Dysfunction in Parkinson's Disease*, Curr. Treat. Options Neurol., **20**(2018), 1–12.

[11] S. Dhar, J. Singh, P. Singh: *Insights into various dysfunctions in Parkinson's disease: a survey*, CSI Trans. ICT, **4**(2016), 117–122.

[12] J. Singh, P. Singh, V. Malik: *Analysis of the Firing Behavior of STN-GPe Network in Parkinson Disease*, Proceedings of the International Conference on Computing and Communication Systems, Springer Singapore, 2018, 791–799.

[13] J. Singh, P. Singh, V. Malik: *Effect of Intrinsic Parameters on Dynamics of STN Model in Parkinson Disease: A Sensitivity-Based Study*, Soft Computing: Theories and Applications, Springer Singapore, 2018, 417–427.

[14] M. D. Humphries, J. A. Obeso, J. K. Dreyer: *Insights into Parkinson's disease from computational models of the basal ganglia*, J. Neurol. Neurosurg. Psychiatry, **89**(11) (2018), 1181–1188.

[15] J. Singh, P. Singh, V. Malik: *Role of Sodium, Potassium and Synaptic Conductance in STN-GPe Model of Basal Ganglia in Parkinson Disease*, Soft Computing: Theories and Applications, Springer Singapore, 2018, 81–95.

[16] J. W. CHOPEK, H. HULTBORN, R. M. BROWNSTONE: *Multistable properties of human subthalamic nucleus neurons in Parkinson's disease*, Proc. Natl. Acad. Sci., **116**(48) (2019), 24326–24333.

[17] T. OTSUKA, T. ABE, T. TSUKAGAWA, W. J. SONG: *Conductance-Based Model of the Voltage-Dependent Generation of a Plateau Potential in Subthalamic Neurons*, J. Neurophysiol., **92**(1) (2004), 255–264.

[18] S. SANTANIELLO, G. FIENGO, L. GLIELMO, W. M. GRILL: *Basal Ganglia Modeling in Healthy and Parkinson's Disease State. I. Isolated Neurons Activity*, American Control Conference, New York, NY, USA, 2007, 4089-4094.

[19] C. HAMMOND, H. BERGMAN, P. BROWN: *Pathological synchronization in Parkinson's disease: networks, models and treatments*, Trends Neurosci., **30**(7) (2007), 357–364.

[20] G. KANG, M. M. LOWERY: *Conductance-based model of the basal ganglia in Parkinson's Disease*, IET Irish Signals and Systems Conference (ISSC 2009), Dublin, Ireland, 2009.

[21] G. KANG, M. M. LOWERY: *A model of pathological oscillations in the basal ganglia and deep brain stimulation in parkinson's disease*, Annual International Conference of the IEEE Engineering in Medicine and Biology Society, 2009, 3909–3912.

[22] D. J. GELB, E. OLIVER, S. GILMAN: *Diagnostic criteria for Parkinson disease*, Arch. Neurol., **56**(1) (1999), 33–39.

[23] K. A. JELLINGER: *Post mortem studies in Parkinson's disease–is it possible to detect brain areas for specific symptoms?*, J. Neural Transm. Suppl., **56**(1999), 1–29, 1999.

[24] T. WICHMANN, M. A. KLIEM, J. SOARES: *Slow oscillatory discharge in the primate basal ganglia*, J. Neurophysiol., **87**(2) (2002), 1145–1148.

[25] M. R. ETZION, O. MARMOR, G. HEIMER, A. RAZ, A. NINI, H. BERGMAN: *Basal ganglia oscillations and pathophysiology of movement disorders*, Curr. Opin. Neurobiol., **16**(6) (2006), 629-637.

[26] A. MORAN, H. BERGMAN, Z. ISRAEL, I. BAR-GAD: *Subthalamic nucleus functional organization revealed by parkinsonian neuronal oscillations and synchrony*, Brain J. Neurol., **131**(12) (2008), 3395–3409.

[27] J. JANKOVIC: *Parkinson's disease: clinical features and diagnosis*, J. Neurol. Neurosurg. Psychiatry, **79**(4) (2008), 368–376.

[28] M. WEINBERGER, W. D. HUTCHISON, A. M. LOZANO, M. HODAIE, J. O. DOSTROVSKY: *Increased gamma oscillatory activity in the subthalamic nucleus during tremor in Parkinson's disease patients*, J. Neurophysiol., **101**(2) (2009), 789-802.

[29] P. SURATHI, K. JHUNJHUNWALA, R. YADAV, P. K. PAL: *Research in Parkinson's disease in India: A review*, Ann. Indian Acad. Neurol., **19**(1) (2016), 9–20.

[30] P. MAITI, J. MANNA, G. L. DUNBAR: *Current understanding of the molecular mechanisms in Parkinson's disease: Targets for potential treatments*, Transl. Neurodegener., **6**(1) (2017), 1–35.

[31] L. MARSILI, G. RIZZO, C. COLOSIMO: *Diagnostic Criteria for Parkinson's Disease: From James Parkinson to the Concept of Prodromal Disease*, Front. Neurol., **9**(2018), 1–10.

[32] D. PARE, R. CURRO'DOSSI, M. STERIADE: *Neuronal basis of the parkinsonian resting tremor: A hypothesis and its implications for treatment*, Neuroscience, **35**(2) (1990), 217–226.

[33] T. WICHMANN, M. R. DELONG: *Oscillations in the basal ganglia*, Nature, **400**(1999), 621–622.

[34] M. D. HUMPHRIES, R. D. STEWART, K. N. GURNEY: *A physiologically plausible model of action selection and oscillatory activity in the basal ganglia*, J. Neurosci. Off. J. Soc. Neurosci., **26**(50) (2006), 12921–12942.

[35] W. J. SONG, Y. BABA, T. OTSUKA, F. MURAKAMI: *Characterization of Ca(2+) channels in rat subthalamic nucleus neurons*, J. Neurophysiol., **84**(5) (2000), 2630–2637.

[36] D. GUEHL ET AL.: *Tremor-related activity of neurons in the 'motor' thalamus: changes in firing rate and pattern in the MPTP vervet model of parkinsonism*, Eur. J. Neurosci., **17**(11) (2003), 2388–2400.

[37] B. R. BREWER, S. PRADHAN, G. CARVELL, A. DELITTO: *Application of modified regression techniques to a quantitative assessment for the motor signs of Parkinson's disease*, IEEE Trans. Neural Syst. Rehabil. Eng. Publ. IEEE Eng. Med. Biol. Soc., **17**(6) (2009), 568–575.

[38] D. AUR, M. JOG, R. R. POZNANSKI: *Computing by physical interaction in neurons*, J. Integr. Neurosci., **10**(4) (2011), 413–422.

[39] J. L. LANCIEGO, N. LUQUIN, J. A. OBESO: *Functional Neuroanatomy of the Basal Ganglia*, Cold Spring Harb. Perspect. Med., 2(12) (2012), 1–21.

[40] A. B. NELSON, A. C. KREITZER: *Reassessing models of basal ganglia function and dysfunction*, Annu. Rev. Neurosci., **37** (2014), 117–135.

[41] J.-S. BRITTAIN, P. BROWN: *Oscillations and the basal ganglia: Motor control and beyond*, NeuroImage, **85**(2) (2014), 637–647.

[42] C. J. WILSON: *Oscillators and Oscillations in the Basal Ganglia*, Neurosci. Rev. J. Bringing Neurobiol. Neurol. Psychiatry, **21**(5) (2015), 530–539.

[43] J. SINGH, P. SINGH, V. MALIK: *Sensitivity analysis of discharge patterns of subthalamic nucleus in the model of basal ganglia in Parkinson disease*, J. Integr. Neurosci., **16**(4) (2017), 441–452.

[44] R. EBERHART, J. KENNEDY: *A new optimizer using particle swarm theory*, in , Proceedings of the Sixth International Symposium on Micro Machine and Human Science, 1995, 39–43.

[45] E. ELBELTAGI, T. HEGAZY, D. GRIERSON: *Comparison among five evolutionary-based optimization algorithms*, Adv. Eng. Inform., **19**(1) (2005), 43-53.

[46] H.-M. FENG: *Self-generation RBFNs using evolutional PSO learning*, Neurocomputing, **70**(1) (2006), 241–251.

[47] J. ZHOU, Z. DUAN, Y. LI, J. DENG, D. YU: *PSO-based neural network optimization and its utilization in a boring machine*, J. Mater. Process. Technol., **178**(1) (2006), 19–23.

[48] F. ZHAO, Z. REN, D. YU, Y. YANG: *Application of An Improved Particle Swarm Optimization Algorithm for Neural Network Training**, International Conference on Neural Networks and Brain, **3**(2005), 1693–1698.

[49] C. ZHANG, H. SHAO: *An ANN's evolved by a new evolutionary system and its application*, Proceedings of the 39th IEEE Conference on Decision and Control (Cat. No.00CH37187), Sydney, NSW, Australia, 2000, 3562–3563.

[50] M. PANT, R. THANGARAJ, A. ABRAHAM: *Particle Swarm Optimization Using Adaptive Mutation*, 19th International Workshop on Database and Expert Systems Applications, 2008, 519–523.

[51] P. SINGH, A. K. YADAV, K. SINGH: *Known-plaintext attack on cryptosystem based on fractional Hartley transform using particle swarm optimization algorithm*, Engineering Vibration, Communication and Information Processing, Springer Singapore, 2019, 317–327.

[52] X.J. FENG, E. S. BROWN, B. GREENWALD, R. KOSUT, H. RABITZ: *Optimal deep brain stimulation of the subthalamic nucleus–a computational study*, J. Comput. Neurosci., **23**(3) (2007), 265–282.

[53] S. T. KITAI, J. M. DENIAU: *Cortical inputs to the subthalamus: intracellular analysis*, Brain Res., **214**(2)(1981), 411–415.

[54] A. NAMBU ET AL.: *Excitatory cortical inputs to pallidal neurons via the subthalamic nucleus in the monkey*, J. Neurophysiol., **84**(1) (2000), 289–300.

[55] F. A. LENZ, H. C. KWAN, R. L. MARTIN, R. R. TASKER, J. O. DOSTROVSKY, Y. E. LENZ: *Single unit analysis of the human ventral thalamic nuclear group Tremor-related activity in functionally identified cells*, Brain, **117**(3) (1994), 531–543.

[56] A. DOVZHENOK, L. L. RUBCHINSKY: *On the Origin of Tremor in Parkinson's Disease*, PLoS ONE, **7**(7) (2012), 2–14.

[57] J. VOLKMANN, M. JOLIOT, E. FAZZINI, U. RIBARY, R. LLINAS: *Central motor loop oscillations in parkinsonian resting tremor revealed by magnetoencephalography*, Neurology, **46**(5) (1996), 1359–1370.

[58] D. TERMAN, J. E. RUBIN, A. C. YEW, C. J. WILSON: *Activity Patterns in a Model for the Subthalamopallidal Network of the Basal Ganglia*, J. Neurosci., **22**(7) (2002), 2963–2976.

[59] J. E. RUBIN, D. TERMAN: *High Frequency Stimulation of the Subthalamic Nucleus Eliminates Pathological Thalamic Rhythmicity in a Computational Model*, J. Comput. Neurosci., **16**(3) (2004), 211–235.

[60] R. POLI, J. KENNEDY, T. BLACKWELL: *Particle swarm optimization*, Swarm Intell., **1**(1) (2007), 33–57.

[61] R. K. SAMALA, M. R. KOTAPURI: *Distributed generation allocation in distribution system using particle swarm optimization based ant-lion optimization*, International Journal of Control and Automation, **13**(1) (2020), 414–426.

[62] N. F. A. AHMAD, S. HARUN, H. N. A. HAMED: *Particle swarm optimization of multilinear regression for evapotranspiration estimation model*, Test Engineering and Management, **81**(2019), 858–866.

DEPARTMENT OF APPLIED SCIENCE
NORTH CAP UNIVERSITY
GURUGRAM, HARYANA, INDIA
E-mail address: srisaitechnologymadurai@gmail.com

DEPARTMENT OF APPLIED SCIENCE
NORTH CAP UNIVERSITY
GURUGRAM, HARYANA, INDIA

DEPARTMENT OF MATHEMATICS
SoET, CENTRAL UNIVERSITY OF HARYANA
MAHENDERGARH, HARYANA, INDIA

IILM ACADEMY OF HIGHER LEARNING
COLLEGE OF ENGINEERING AND TECHNOLOGY
GREATER NOIDA, UTTAR PRADESH, INDIA

AMITY SCHOOL OF APPLIED SCIENCES
AMITY UNIVERSITY HARYANA
GURUGRAM, INDIA